Numerical Study on NO Emission with Flue Gas Dilution in Air and Fuel Sides

Eun-Seong Cho, Suk Ho Chung*
School of Mechanical and Aerospace Engineering, Seoul National University, Seoul 151-744, Korea

Flue gas recirculation (FGR) is widely adopted to control NO emission in combustion systems. Recirculated flue gas decreases flame temperature and reaction rate, resulting in the decrease in thermal NO production. Recently, it has been demonstrated that the recirculated flue gas in fuel stream, that is, the fuel induced recirculation (FIR), could enhance much improved reduction in NO per unit mass of recirculated gas, as compared to conventional FGR in air. In the present study, the effect of dilution methods in air and fuel sides on NO reduction has been investigated numerically by using N_2 and CO_2 as diluent gases to simulate flue gases. Counterflow diffusion flames were studied in conjunction with the laminar flamelet model of turbulent flames. Results showed that CO_2 dilution was more effective in NO reduction because of large temperature drop due to the larger specific heat of CO_2 compared to N_2. Fuel dilution was more effective in reducing NO emission than air dilution when the same recirculation ratio of dilution gas was used by the increase in the nozzle exit velocity, thereby the stretch rate, with dilution gas added to fuel side.

Key Words : Flue Gas Recirculation (FGR), Fuel Induced Recirculation (FIR), Nitric Oxides, Counterflow

1. Introduction

Combustion efficiency and clean combustion are the two main issues in recent fossil energy utilization. The control of nitrogen oxides (NO_x) has been a major issue in designing combustion systems, since NO_x play a key role in ozone depletion and the generation of photochemical smog (Ahn et al., 2002; Cho et al., 2003). Due to the temperature sensitive NO_x production mechanism, decreasing flame temperature is a viable method in suppressing thermal NO_x formation.

Lean premix combustion and low oxygen combustion which decrease oxygen concentration in oxidizer by inert gas dilution are practical methods to reduce flame temperature (Wünning, 1997; Sohn et al., 2002). Especially, flue gas recirculation (FGR) is one of the well-known methods to control NO_x emission (Beer, 1996; Arai, 2000). A portion of exhaust gas is recirculated in oxidizer (air) side in FGR, which decreases flame temperature and reduces NO_x emission, since combustion takes place in relatively low oxygen environment. This method has been applied in utility and industrial boilers. When applied to automotive engines, this method is frequently called exhaust gas recirculation (EGR).

FGR generally requires large amount of flue gases for the effective control of NO_x, thus requires a large induced draft fan. In such a case, flame instability may occur due to the increase in oxidizer velocity.

To resolve this problem, fuel induced recirculation (FIR) method was introduced to reduce NO_x emission with less amount of flue gas than

* Corresponding Author,
E-mail : shchung@snu.ac.kr
TEL : +82-2-880-7114; **FAX** : +82-2-889-1842
School of Mechanical and Aerospace Engineering, Seoul National University, Seoul 151-744, Korea.
(Manuscript **Received** December 1, 2004; **Revised** April 15, 2005)

FGR (Feese and Turns, 1998 ; Lang, 1994). This method recirculates flue gas in the fuel-side instead of air-side. Chemical kinetic study of fuel and air dilution has been preformed in high temperature conditions (Choi and Katsuki, 2002).

An experimental study shows that comparable NO reduction effect can be achieved with relatively small amount of flue gas in FIR as compared to FGR and a high velocity FIR case has appreciable NO reduction (Cho and Chung, 2004). Based on a simple heat capacity analysis, the reduction in flame temperature resulting from recirculated flue gas should not depend on whether the flue gas is diluted in the air or fuel sides. Considering this, the effectiveness of FIR is noteworthy.

The object of the present study is to investigate the effectiveness of flue gas dilution in counterflow diffusion flames numerically by adopting a detailed chemistry model. The flue gas is simulated as N_2 or CO_2 by supplying them either in air-side or fuel-side, to identify the effects of FGR and FIR on NO reduction.

2. Governing Equations and Numerical Analysis

A counterflow diffusion flame offers a convenient geometry in modeling the detailed processes that occur in diffusion flames. The governing equations of continuity, momentum, energy, and species in the boundary layer formulation for an axisymmetric counterflow are as follows ;

$$\frac{dV}{dy}+2a\rho f'=0 \tag{1}$$

$$\frac{d}{dy}\left(\mu\frac{df'}{dy}\right)-V\frac{df'}{dy}+a[\rho_\infty-\rho(f')^2]=0 \tag{2}$$

$$\frac{d}{dy}\left(\lambda\frac{dT}{dy}\right)-C_pV\frac{dT}{dy}-\sum_{k=1}^{K}\rho Y_kV_{ky}C_{pk}\frac{dT}{dy}-\sum_{k=1}^{n}\omega_kW_kh_k=0 \tag{3}$$

$$\frac{d}{dy}(\rho Y_kV_{ky})+V\frac{dY_k}{dy}-\omega_kW_k=0,\quad k=1,\cdots,K \tag{4}$$

where u, v and x, y are the transverse and axial velocities and coordinates, respectively ; ρ is the density ; f is the stream function defined as $u=u_\infty(x)f'(y)$; ∞ is the free-stream condition, V is the axial mass flux ρv ; T is the temperature ; Y_k, W_k, ω_k, C_{pk}, and h_k are the mass fraction, the molecular weight, the reaction rate, the specific heat, and the enthalpy of k-th species, respectively ; C_p is the mixture specific heat ; a is the strain rate with $u_\infty=a_\infty x/2$ and $v_\infty=-a_\infty y$; κ is the stretch rate which is $2a_\infty$ in axisymmetric counterflow, N is the number of species involved ; V_{ky} is the diffusion velocity of k-th species in direction determined from the Curtiss-Hirshfelder approximation ; and λ and μ are the thermal conductivity and the viscosity from the Wilke's formula, respectively. Thermodynamic and transport properties are calculated from the CHEMKIN III (Kee et al., 1996) and the TRANSPORT PACKAGE (Kee et al., 1986), respectively. The equation of state is $p=\rho RT/\bar{W}$, where p is the pressure, $\bar{W}$ is the average molecular weight, and R is the gas constant.

The boundary conditions are

$$\text{at } y=-L,\ : f'=0,\quad Y_k=Y_{k,F},\ k=1,\ 2,\ \cdots,\ K,\quad T=T_F,\quad V=V_F \tag{5}$$

$$\text{at } y=L,\ : f'=0,\quad Y_k=Y_{k,O},\ k=1,\ 2,\ \cdots,\ K,\quad T=T_O,\quad V=V_O \tag{6}$$

where the plug flow is assumed in the free stream and F and O indicate fuel and oxidizer stream, respectively. The numerical calculation adopts discretization, the modified Newton iteration, and the Euler time integration (Giovangigli and Smooke, 1987) with grid smoothing for improving convergence (Lee and Chung, 1994).

A detailed chemical mechanism has been adopted the GRI 3.0 mechanism which covers 53 species and 325 elementary reactions including NO related reactions (Smith et al., 2000).

The presence of dilution, or recirculated gases, is taken into account by specifying the species mole fractions at both the fuel-side boundary

(FIR) and oxidizer-side boundary (FGR).

3. Results and Discussion

Two types of dilution conditions were calculated using N_2 or CO_2 as diluent. And two types of flow conditions were tested : (1) variable dilution with fixed velocity (FV) of 50 cm/s for all cases and (2) variable dilution with fixed flowrate (FF) of air for FGR or fuel for FIR condition to simulate the experiment (Cho and Chung, 2004). This second condition of fixed flowrate was achieved by increasing the velocity at either the fuel or oxidizer nozzle where the diluent was added. The test fuel was propane (C_3H_8).

3.1 Flame structure

To evaluate the effectiveness of FGR and FIR, the recirculation ratio (RR) is introduced as follows. It is typically the same as the definition of the FGR ratio.

$$\mathrm{RR}(\%)=\frac{\text{mole of diluent } (N_2,\ CO_2)}{\text{mole of stoichiometric mixture}}\times 100 \tag{7}$$

This parameter can also be expressed in terms of the mole fractions of propane (oxygen) in the fuel (oxidizer) stream, X_F (X_{02}) as

$$RR=f_s\frac{1-X_F}{X_F}+(1-f_s)\frac{0.21-X_{02}}{X_{02}} \tag{8}$$

where f_s is the stoichiometric mixture fraction (mole of fuel per mole of air in the stoichiometric mixture) and is 0.04 for propane.

For FGR (FIR) case, $X_F(X_{02})$ is set to unity (0.21) and $X_{02}(X_F)$ can be varied to simulate the typical range RR.

Typical profiles of the temperature and species mole fractions for (a) FGR (X_{02}=0.19) and (b) FIR (X_F=0.285) with N_2 dilution are shown in Fig. 1. Both cases have the same RR of 10% and the fuel velocity (V_F) and oxidizer velocity (V_O) are both 50 cm/s. Even though the fuel and nitrogen profiles are quite different, the profiles of temperature and the production species such as CO_2, H_2O, and NO are qualitatively similar.

3.2 Comparison of FGR and FIR

Figure 2 shows the adiabatic (T_{ad}) and maximum flame temperature (T_{max}) of the N_2 and CO_2 dilution cases with RR for the fixed velocity condition. The adiabatic flame temperature was calculated from the Chemical Equilibrium Calculation (CEC) code (Gordon and McBride, 1971). FGR and FIR conditions are calculated from counterflow condition under the stretch rate of 100 s^{-1} since the flame temperature is lower than zero stretch case of CEC calculation. The T_{ad} and T_{max} for both the FGR and FIR decrease with RR and the slopes of T_{ad} and T_{max} with RR are similar. The FIR case shows lower T_{max} than the FGR case for the same RR. This implies that the fuel dilution can be more effective than oxidizer dilution in reducing the peak

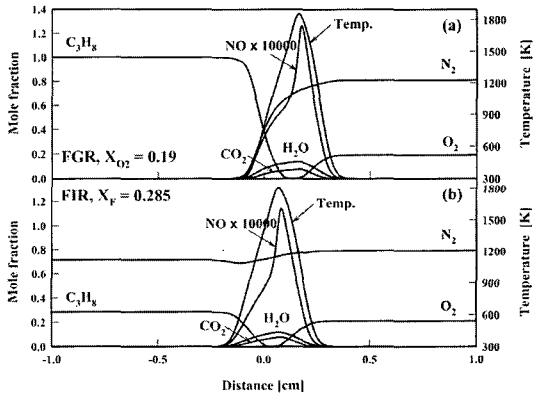

Fig. 1 Temperature and species molefractions in (a) FGR and (b) FIR conditions

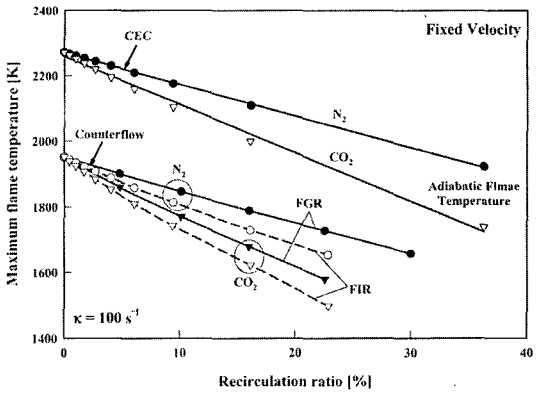

Fig. 2 Adiabatic and maximum flame temperatures with recirculation ratio in fixed velocity cases

temperatures. As compared to the N_2 dilution, the CO_2 dilution case shows appreciable decrease in the T_{max} because of the higher specific heat.

The characteristics of NO production can be represented by the emission index of NO (EINO) following the procedure of Takeno and Nishioka (1993), which is defined in terms of the NO production rate, $\dot{\omega}_{NO}$, and the fuel consumption rate, $-\dot{\omega}_F$ as :

$$EINO=\frac{\int_{-L}^{L}\dot{\omega}_{NO}W_{NO}dx}{\int_{-L}^{L}\dot{\omega}_F W_F dx} \tag{9}$$

where W_{NO} and W_F are the molecular weights of nitric oxide and propane, respectively.

Figure 3 shows the EINO in the fixed velocity case. The NO reduction with the CO_2 dilution is more effective than the N_2 dilution, because of larger specific heat in reducing flame temperature. In the case of CO_2 dilution, X_{O2}=0.17 (RR=22.6%) shows about 90% NO reduction as compared to the base condition of X_{O2}=0.21 (RR=0%).

The EINO decreases with the RR except for the FIR with N_2 dilution. It shows that EINO increases for small RR and decreases for RR > 10%. This trend agrees with the previous research (Choi and Katsuki, 2002), where the behavior has been explained by the existence of nitrogen in the fuel stream.

The results of the EINOs having larger values for the FIR compared to the FGR case for both the N_2 and CO_2 dilutions are contrary to the experimental findings of Cho and Chung (2004). Therefore further analyses are required. In determining EINO, both the fuel consumption rate and NO production rate are required. Figure 4 shows the fuel consumption rate, NO production rate, and EINO with the RR for $V_F = V_O$= 50 cm/s of fixed velocity case with the N_2 dilution. The fuel consumption rates decrease with RR and especially the decrease for the FIR case are appreciable because of the decrease in propane flow rate with RR. Since the NO production rates are nearly the same together with the rapid decrease in the fuel consumption rate, the EINO for the FIR case shows increasing trend for small RR. The experimental results in jet diffusion flames with fixed fuel jet velocity show that the NO production rates were comparable for both the FIR and FGR cases (Cho and Chung, 2004).

In a practical swirl burner, when FIR is adopted, the fuel jet velocity will increase. To evaluate this effect, the cases with fixed flowrate (FF) were tested. For the FGR (FIR) case, V_F (V_O) is fixed and V_O (V_F) is varied with the dilution. The results of the fuel consumption rates and NO

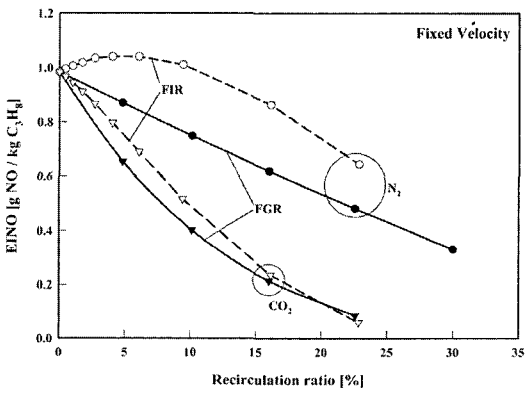

Fig. 3 EINO with recirculation ratio in fixed velocity case

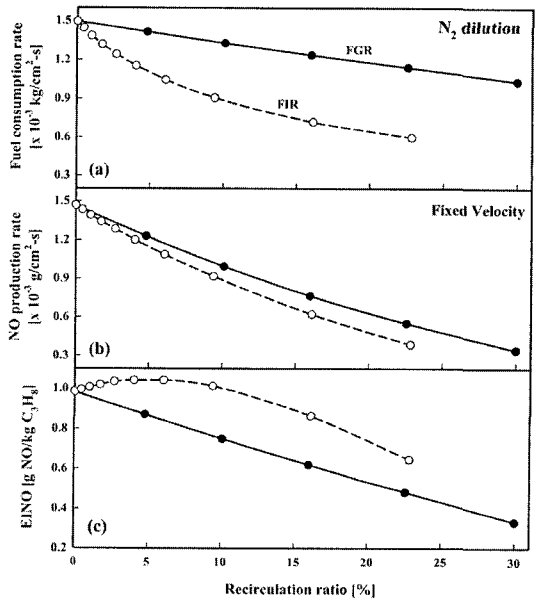

Fig. 4 Fuel consumption rate, NO production rate, and EINO with recirculation ratio in N_2 diluted fixed velocity case

production rates are shown in Fig. 5. The fuel consumption rate with RR in N_2 dilution show comparable trend for both the FGR and FIR cases since the propane flowrate are the same. Whereas the NO production rate rapidly decreased with RR for the FIR case. In the cases of FF-FIR, higher RR conditions could not be achieved because of flame extinction.

Figure 6 shows T_{max} and EINO with RR for the fixed flowrate cases. The maximum temperature for the FIR cases decrease rapidly with RR as compared to the fixed velocity cases shown in Fig. 2. As a consequence, the trend of EINO decreases rapidly for RR≥5% as compared to the FGR cases. This result is in qualitative agreement with the experimental data (Cho and Chung, 2004). The reason being that is although the fuel consumption rate decreases with RR, the decrease in T_{max} results in the rapid reduction in the EINO.

Although not shown, T_{max} and EINO for the FGR with the fixed velocity and fixed flowrate cases are nearly the same, since the increase in the oxidizer velocity is not influenced much by the dilution as compared to the FIR case. For example, X_{O2}=0.16 (RR=30%), V_O=66 cm/s as compared to 50 cm/s for X_{O2}=0.21 (RR=0%). For the FIR case, however, the increase in V_F is significant with RR. For example, V_F=200 cm/s for X_F=0.25 (RR=12%) as compared to V_F=50 cm/s for X_F=1.0 (RR=0%). Consequently the temperature and EINO are much influenced by RR.

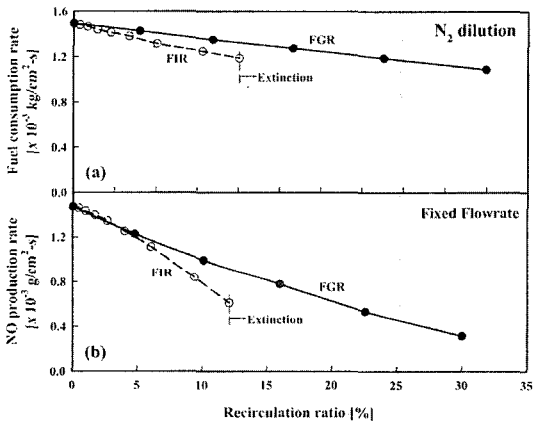

Fig. 5 Fuel consumption and NO production rates with recirculation ratio in N_2 diluted fixed flowrate case

3.3 NO formation characteristics

NO production could be affected by stretch rate, dilution ratio, and diluent species. To evaluate the effectiveness of each NO mechanism for total EINO with RR, NO formation chemistry is further analyzed. The thermal and prompt NO mechanisms (Nishioka et al., 1994) contributing to the NO formation are shown in Fig. 7 with RR for the case of fixed flowrate with N_2 dilution. Both the FGR and FIR have similar trend in that the thermal NO mechanism decrease with RR because the thermal mechanism dominantly

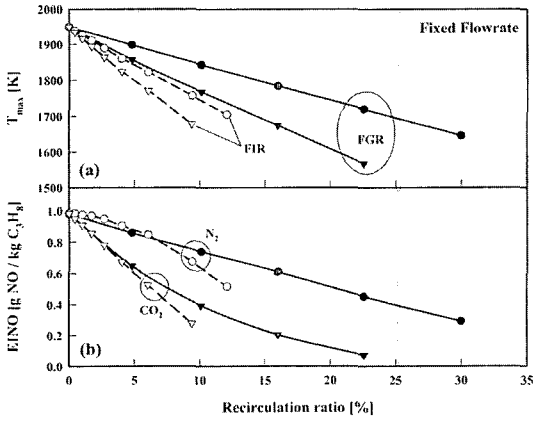

Fig. 6 Maximum flame temperature and EINO with recirculation ratio in fixed flowrate case

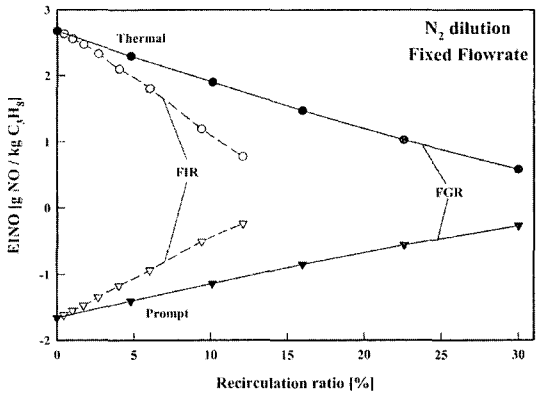

Fig. 7 Thermal and prompt NO contribution to EINO with recirculation ratio

affected by flame temperature. On the contrary, the prompt mechanism shows inverse trend that the prompt EINO increases with RR which reason is not clear yet. This paper just demonstrated the trend of thermal and prompt NO with RR. The CO_2 dilution case has the similar trend even though the trend with RR is more sensitive.

The fixed flowrate case is more effective than fixed velocity case because of the fuel or oxidizer velocities which increase stretch rate and decrease flame temperature with RR. To exclude this effect, the stretch rate is fixed at 100 s^{-1} and the NO formation characteristics were analyzed by comparing the cases of N_2 and CO_2 dilutions in fuel and air sides.

The NO production rate with N_2 and CO_2 dilutions in the FGR and FIR conditions are shown in Fig. 8 for fixed RR of 10%, which are X_{O2}= 0.19 in the FGR case and X_F=0.285 in the FIR case. The results show that the profiles have qualitatively similar shape and CO_2 dilution has lower peak production rate than N_2 and FIR case shows lower peak value than FGR.

To further illustrate the similarity between the N_2 and CO_2 dilutions in the FIR condition. These rates are normalized and the result is shown as the insert in Fig. 8. It shows that the shapes of profiles are nearly the same, implying that the N_2 or CO_2 dilution effects on NO production rate are similar.

The contribution of each reaction step on the integrated NO production rate for N_2 or CO_2 dilutions at the same RR for the FGR and FIR conditions is shown in Fig. 9. Even though the magnitude of each reaction step for the integrated NO production rate is different, the role of production (positive) and consumption (negative) reaction steps and their importance are similar. It means that each reaction step related to NO production is not differ much whether the air side or fuel side dilution and whether the N_2 or CO_2 dilution.

The thermal NO mechanisms show positive production rates except $N_2+O=N+NO$ reaction. For the prompt NO mechanisms, $HNO+H=H_2+NO$ reaction shows very high positive NO production rate and $HCNO+CO=HCCO+NO$ reaction appreciable negative NO production rate.

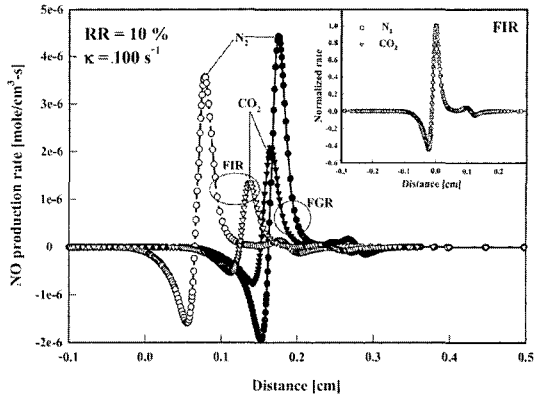

Fig. 8 NO production rate at same stretch rate and recirculation ratio

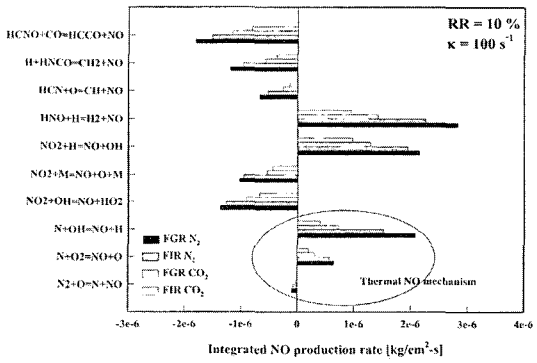

Fig. 9 Integrated NO production rate for each reaction steps

4. Conclusions Remarks

The following conclusions can be drawn in the FGR and FIR cases.

(1) The maximum flame temperature and EINO are reduced by the decrease in oxidizer concentration in the FGR condition. CO_2 dilution is more effective in the reduction of NO than N_2 because of its higher specific heat. In the cases of fixed velocity and fixed flowrate FGR conditions, the results are comparable because the oxidizer velocity is not affected much.

(2) The NO emission ratio decreased with the dilution ratio in the FIR conditions. The fixed flowrate case is more effective in NO reduction

than the fixed velocity case, because of increasing nozzle exit velocity with dilution. Consequently, the flame temperature and NO production can be decreased.

(3) Comparing the FGR and FIR conditions, the FIR case is more effective in NO reduction with small amounts of dilution than the FGR case even though the EINO almost same within 5% of RR. The FGR and FIR have nearly the same effect in NO reduction ratio in the fixed velocity conditions, implying that the flow velocity has significant role in NO reduction.

Acknowledgments

This work was supported by the Korea Aerospace Research Institute (KARI) and the Combustion Engineering Research Center (CERC).

References

Ahn, K. Y., Kim, H. S., Son, M. K., Kim, H. K. and Kim, Y. M., 2002, "An Experimental Study on the Combustion Characteristics of a Low NO_x Burner Using Reburning Technology," *KSME Int'l J.*, Vol. 16, No. 7, pp. 950~958.

Arai, M., 2000, "Flue Gas Recirculation for Low NOx Combustion System," *IJPGC2000-15073*, pp. 1~10.

Beer, J. M., 1996, "Low NO_x Burners for Boilers, Furnaces, and Gas Turbines; Drive Towards the Low Bonds of NO_x Emissions," *Combust Sci. and Tech.*, Vol. 121, pp. 169~191.

Cho, E. -S., Sung, Y., and Chung, S. H., 2003, "An Experiment on Low NO_x Combustion Characteristics in a Multi-Staged Burner," *Trans. of KSME (B)*, Vol. 27, No. 1, pp. 32~38.

Cho, E. -S. and Chung, S. H., 2004, "Characteristics of NO_x Emission with Flue Gas Dilution in Air and Fuel Sides," *KSME Int'l J.*, Vol. 18, No. 12, pp. 2302~2308.

Choi, K. -M. and Katsuki, M., 2002, "Chemical Kinetic Study on the Reduction of Nitric Oxide in Highly Preheated Air Combustion," *Proc. of Comb. Institute*, Vol. 29, pp. 1165~1171.

Feese, J. J. and Turns, S. R., 1998, "Nitrogen Oxide Emission from Laminar Diffusion Flames: Effects of Air-Side versus Fuel-Side Dilution Addition," *Combust. Flame*, Vol. 113, pp. 66~78.

Lang, J., 1994, "Low NO_x Burner Design Achieves Near SCR Levels," *ASME*, PWR-Vol. 24, pp. 127~131.

Nishioka, M., Nakagawa, S., Ishikawa, Y., and Takeno, T., 1994, "NO Emission Characteristics of Methane-Air Double Flame," *Combust. Flame*, Vol. 98, pp. 127~138.

Wünning, J. A. and Wünning, J. G., 1997, "Flamless Oxidation to Reduce Thermal NO-Formation," *Prog. Energy Combust. Sci.*, Vol. 23, pp. 81~94.

Giovangigli, V. and Smooke, M. D., 1987, "Calculation of Extinction Limits for Premixed Laminar Flames in a Stagnation Flames in a Stagnation Points Flow," *J. Comp. Phys.*, Vol. 68, pp. 327~345.

Gordon, S. and McBride, B. J., 1971, "Computer Program for Calculation of Complex Chemical Equilibrium Compositions, Rocket Performance, Incident and Reflected Shock, and Chapman-Jouguet Detonations," *NASA SP-273*, Washington D.C.

Lee, S. D. and Chung, S. H., 1994, "On the Structure and Extinction of Interacting Lean Methane/Air Premixed Flames," *Combust. Flame*, Vol. 98, pp. 80~92.

Kee, R. J., Ruply, F. M., and Miller, J. A., 1996, "CHEMKIN-III: A Fortran Chemical Kinetics Package for the Analysis of Gas-Phase Chemical and Plasma Kinetics," *SAND 96-8216*, Sandia National Laboratories Report.

Kee, R. J., Dixon-Lewis, G., Warnatz, J., Coltrin, M. E., and Miller, J. A., 1986, "A Fortran Computer Code Package for the Evaluation of Gas-Phase Multicomponent Transport Properties," *SAND 86-8246*, Sandia National Laboratories Report.

Smith, G. P., Golden, D. M., Frenklach, M., Moriarty, N. W., Eiteneer, B., Goldenberg, M., Bowman, C. T., Hanson, R. K., Song, S., Gardiner Jr., W. C., Lissianski, V. V., and Qin, Z., 2000, "Gri-Mech 3.0," http://www.me.berkeley.edu/ gri_mech/.

Sohn, C. H., Jeong, I. M., and Chung, S. H.,

2002, "Numerical Study of the Effects of Pressure and Air-Dilution on NO Formation in Laminar Counterflow Diffusion Flames of Methane in High Temperature Air," *Combust. Flame*, Vol. 130, pp. 83~93.

Takeno, T. and Nishioka, M., 1993, "Species Conservation and Emission Indices for Flames Described by Similarity Solutions," *Combust. Flame*, Vol. 92, pp. 465~468.